

# Correction of the retinal dystrophy phenotype of the RCS rat by viral gene transfer of *Mertk*

Douglas Vollrath\*<sup>†</sup>, Wei Feng\*, Jacque L. Duncan<sup>‡</sup>, Douglas Yasumura<sup>‡</sup>, Patricia M. D'Cruz\*, Aimee Chappelow<sup>‡</sup>, Michael T. Matthes<sup>‡</sup>, Mark A. Kay\*, and Matthew M. LaVail<sup>‡</sup>

\*Department of Genetics, Stanford University School of Medicine, Stanford, CA 94305-5120; and <sup>‡</sup>Departments of Anatomy and Ophthalmology, University of California, San Francisco School of Medicine, San Francisco, CA 94143-0730

Edited by Jeremy Nathans, Johns Hopkins University School of Medicine, Baltimore, MD, and approved August 14, 2001 (received for review July 16, 2001)

The Royal College of Surgeons (RCS) rat is a widely studied animal model of retinal degeneration in which the inability of the retinal pigment epithelium (RPE) to phagocytize shed photoreceptor outer segments leads to a progressive loss of rod and cone photoreceptors. We recently used positional cloning to demonstrate that the gene *Mertk* likely corresponds to the retinal dystrophy (*rdy*) locus of the RCS rat. In the present study, we sought to determine whether gene transfer of *Mertk* to a RCS rat retina would result in correction of the RPE phagocytosis defect and preservation of photoreceptors. We used subretinal injection of a recombinant replication-deficient adenovirus encoding rat *Mertk* to deliver the gene to the eyes of young RCS rats. Electrophysiological assessment of animals 30 days after injection revealed an increased sensitivity of treated eyes to low-intensity light. Histologic and ultrastructural assessment demonstrated substantial sparing of photoreceptors, preservation of outer segment structure, and correction of the RPE phagocytosis defect in areas surrounding the injection site. Our results provide definitive evidence that mutation of *Mertk* underlies the RCS retinal dystrophy phenotype, and that the phenotype can be corrected by treatment of juvenile animals. To our knowledge, this is the first demonstration of complementation of both a functional cellular defect (phagocytosis) and a photoreceptor degeneration by gene transfer to the RPE. These results, together with the recent discovery of *MERTK* mutations in individuals with retinitis pigmentosa, emphasize the importance of the RCS rat as a model for gene therapy of diseases that arise from RPE dysfunction.

The Royal College of Surgeons (RCS) rat strain displays an unusual retinal phenotype in which shed photoreceptor (PR) outer segment (OS) debris accumulates in the subretinal space (1). PR disk shedding normally commences at postnatal day (P)12 in the rat (2), and an OS debris layer is readily apparent in the eyes of RCS animals at P20. Genetic chimera studies suggest that the defect is a cell-autonomous function of the RPE, not the PRs (3). Indeed, *in vivo* (4) and RPE cell culture studies (5) revealed a defect in the ability of RCS RPE to phagocytize shed OS membranes. Despite the RPE-specific nature of the defect, death strikes the PRs first, through the process of apoptosis (6). The time course of PR degeneration is rapid, beginning around P20, with few PR nuclei remaining in the outer nuclear layer (ONL) by P60. Thinning and atrophy of the RPE begins after onset of PR degeneration. The cause of PR cell death is not well understood; the debris zone acting as a diffusion barrier to metabolites (7), disruption of the interphotoreceptor matrix (8), and PR hypoxia due to diminished oxygen diffusion (9) have been proposed as explanations.

In contrast to the extensively studied retinal phenotype of the RCS rat, the nature of the genetic defect has remained obscure until recently. Early genetic linkage studies showed that the phenotype is completely recessive and segregates as a single Mendelian locus (10) named *rdy* (11). *CD36* was proposed as a candidate for *rdy* on the basis of its apparent role in RPE phagocytosis (12) and evidence that it is abnormally expressed in the RCS retina (13). We recently used a positional cloning

approach to identify a telltale mutation in the RCS allele of the gene for the receptor tyrosine kinase *Mertk* (also known as *Mer*) (14). The RPE is the major site of expression of *Mertk* in the rat retina (14). We found a small deletion of genomic DNA in the RCS rat that included part of the second coding exon. The deletion results in production of an aberrant mRNA in which the second coding exon has been skipped, leading to a frameshift and premature stop signal 20 codons after the start of the ORF. This severe disruption of a gene that normally encodes a 994-aa protein is almost certainly a null mutation.

Conclusive evidence that *Mertk* is the gene for *rdy* requires genetic complementation of the defect, made feasible by the loss-of-function nature of the RCS *Mertk* mutation. Germline transgenesis has been used to complement two mouse retinal degeneration mutations (15, 16), but rat transgenic technology is more costly and not as widely used as that for mouse. We therefore chose to address the problem by somatic gene transfer with a viral vector. Viral gene replacement therapy has been used in a number of animal models of retinal degeneration caused by PR (17–20) or RPE (21, 22) defects. Successful complementation of the *rdy* phenotype would also serve as a model for treatment of individuals with retinitis pigmentosa who harbor *MERTK* mutations (23) and, more generally, other diseases in which the RPE is dysfunctional, such as age-related macular degeneration.

## Materials and Methods

**Recombinant Adenovirus.** A cDNA clone containing the entire coding region of rat *Mertk* was isolated by reverse transcription-PCR (RT-PCR), with oligonucleotide primers from the 5' (AGAAGTCCAGATCCGC) and 3' (GGCTGGTCTCATCAGAA) untranslated regions of rat *Mertk* and cDNA generated from the neural retina of wild-type RCS-*rdy*<sup>+</sup> animals (24). The resulting 3,019-bp PCR product was cloned into pUC18. Multiple clones were sequenced, and portions of two clones were combined at the only *Bam*HI site in the coding region to create a *Mertk* cDNA clone free of PCR-induced errors.

An expression cassette was created by subcloning the *Mertk* cDNA between the *Hind*III and *Eco*RI sites of pCDNA3 (Invitrogen), thereby placing it downstream of a cytomegalovirus (CMV) promoter and upstream of a simian virus 40 polyadenylation signal. The cassette was excised with *Dra*III and *Nru*I, subcloned into pΔE1sp1A (25), and the resulting plasmid was cotransfected with pJM17 (26) into 293 cells (27). Viral plaques were screened by restriction mapping and Southern blot hybrid-

This paper was submitted directly (Track II) to the PNAS office.

Abbreviations: PR, photoreceptor; OS, outer segment; P, postnatal day; RPE, retinal pigment epithelium; STR, scotopic threshold response; RT-PCR, reverse transcription-PCR; ONL, outer nuclear layer; ERG, electroretinography; Exp., experiment.

<sup>†</sup>To whom reprint requests should be addressed. E-mail: vollrath@genome.stanford.edu.

The publication costs of this article were defrayed in part by page charge payment. This article must therefore be hereby marked "advertisement" in accordance with 18 U.S.C. §1734 solely to indicate this fact.

**Table 1. Summary of experiments**

Experiment	Strain	Age injected-taken	n	Experimental eye	Control eye
1	RCS	P22-P52	3	Stock Ad- <i>Mertk</i> *	Ad- <i>GFP</i> or UI
2	RCS	P23-P26, 30, 37, 51, or 85	12	Stock Ad- <i>Mertk</i> *	Ad- <i>GFP</i> or UI
3	WT	P24-P27, 31, 38, or 52	4	Stock Ad- <i>Mertk</i> *	Ad- <i>GFP</i> or UI
4	RCS	P25-P52	10	Diluted Ad- <i>Mertk</i> <sup>†</sup>	Stock* or diluted <sup>†</sup> vehicle
5	RCS	P23-P55, 56, or 57	10	Diluted Ad- <i>Mertk</i> <sup>†</sup>	Stock* or diluted <sup>†</sup> vehicle
6	RCS	P25-P57, 58, or 59	10	Dialyzed Ad- <i>Mertk</i>	PBS or UI

UI, uninjected; WT, wild-type RCS-*rdy*<sup>+</sup> strain.

\*In 10% glycerol.

<sup>†</sup>In 1% glycerol.

ization, and a replication-deficient (E1 gene-deleted), recombinant adenovirus (Ad-*Mertk*) was amplified by standard methods (28). After two rounds of purification by CsCl gradient centrifugation, the viral preparation was dialyzed overnight against a buffer containing 1 mM MgCl<sub>2</sub>, 10% glycerol, and 10 mM Tris, pH 7.5. The titer of the purified viral stock was  $1 \times 10^{11}$  plaque-forming units/ml. PCR amplification of viral-infected HeLa cell lysate with primers from the E1 gene showed no evidence of wild-type virus. Aliquots of viral stock were stored at  $-80^{\circ}\text{C}$  and thawed immediately before use. An adenovirus that expresses green fluorescent protein under control of a CMV promoter, Ad-*GFP* (Quantum, Montreal), the same serotype as Ad-*Mertk* (Ad5), was used as a control in some experiments.

**RT-PCR.** HeLa cells were grown to 80% confluence before exposure to Ad-*Mertk* for 24 or 48 h. After infection, total RNA was isolated, digested with DNase I (Boehringer Mannheim), and reverse transcribed into cDNA by using random hexamers and SuperScript II reverse transcriptase (Invitrogen). A 560-bp fragment of rat *Mertk* (14) was amplified for 30 cycles at a  $60^{\circ}\text{C}$  annealing temperature with primers (CAACACCGAGTCTATGCTCA; ACAGGAAGGTGTGGAGGTCT) that did not cross-amplify human *MERTK*. To assess wild-type *Mertk* expression in treated animals, a 378-bp fragment was amplified for 35 cycles with primers from the second (CATGGTGGAAAGATGGAAAG) and third (TCAGACCAGGTACGGTTAGG) coding exons at a  $60^{\circ}\text{C}$  annealing temperature.

**Immunoblotting.** HeLa cells were infected with purified Ad-*Mertk* or Ad-*GFP* at a multiplicity of infection of 10 for 42 h. Cells were lysed in loading buffer, and proteins were separated on a 6% SDS-PAGE gel and transferred to nitrocellulose. The membrane was probed with a 1:1,000 dilution of a polyclonal antibody directed against rat *Mertk* (W.F., D.Y., M.T.M., M.M.L., and D.V., unpublished work).

**Animals and Subretinal Injection of Adenovirus.** Pink-eyed inbred RCS rats and congenic RCS-*rdy*<sup>+</sup> rats wild-type at the *rdy* locus (24) were maintained in a 12-hr light/12-hr dark environment of less than 15 lux (1 footcandle = 10.76 lx) illuminance. At different ages soon after weaning and before significant PR degeneration (Table 1), 2  $\mu\text{l}$  of viral suspension was delivered to the subretinal space in the superior hemisphere of one eye of anesthetized rats, as described elsewhere (29). The contralateral eye was either uninjected or injected with a control (Table 1). All procedures adhered to the Association for Research in Vision and Ophthalmology Resolution on the Use of Animals in Research.

**Histological Analysis.** One-micrometer-thick sections were made along the vertical meridian (30) from perfusion-fixed eyes that had been postfixed in osmium tetroxide and embedded in epoxy resin. Sections were stained with toluidine blue. The thickness of

the ONL, a measure of PR number (31), was obtained as described (32) by making 54 measurements (three at each of 18 contiguous fields) around the entire retinal section. For statistical analysis, each treatment group was compared with appropriate controls (Table 1) by using Student's two-tailed *t* test. For electron microscopy, 1.5- $\mu\text{m}$  epoxy-embedded sections from selected blocks were re-embedded, and thin sections were cut and stained with uranyl acetate/lead citrate.

**Electroretinographic Analysis.** Electroretinography (ERG) was performed by using contact lens electrodes for rats (33) essentially as described (34) with the following exceptions. After dark adaptation overnight and preparation in dim red light, rats were dark adapted an additional 45 min and monitored with an infrared camera. By using a UTAS-E 3000 Visual Diagnostic System (LKC Technologies, Gaithersburg, MD) and beginning below ERG threshold, stimuli were presented in order of increasing luminance from  $-5.6$  to  $+2.4$  log cd·s/m<sup>-2</sup>. Several responses at each intensity were computer averaged. Interstimulus intervals ranged from 5 seconds at the lowest intensities to 240 seconds at the highest intensities. Threshold criterion amplitude was 10  $\mu\text{V}$  for a-waves and 20  $\mu\text{V}$  for scotopic threshold responses (STRs) and b-waves.

## Results

**A Recombinant Adenovirus Expresses Rat *Mertk*.** We chose adenovirus as an initial vector for delivery of *Mertk* to the RCS rat retina for several reasons. The *rdy* defect resides in the RPE (3), and adenovirus can efficiently transfer genes to mouse RPE, in comparison to PRs (35, 36). Adenovirus-mediated gene transfer can achieve immediate and strong RPE expression that persists for as much as 6 weeks (35), closely matching the rapid degeneration in RCS rats. Moreover, adenovirus had been used to transfer the gene encoding basic fibroblast growth factor to the RPE of RCS rats with therapeutic effect (37). The CMV promoter was chosen because of its demonstrated efficacy in the RPE (35, 36). A recombinant adenovirus with a rat *Mertk* cDNA under control of a CMV promoter was constructed and purified by standard methods. Expression of *Mertk* was confirmed by assaying mRNA and protein isolated from cultures of infected cells (Fig. 1).

**Viral-Mediated Expression Throughout Experimental Period.** To assess the location, magnitude, and persistence of adenovirus-mediated expression in our study, we injected Ad-*GFP* into the eyes of RCS rats [Table 1, Experiments (Exp.) 1 and 2] and observed strong expression by fluorescence microscopy in the RPE (but not elsewhere in the retina) throughout the experimental period, 3 and 28 days after injection (data not shown), consistent with previous reports (35, 37). At both ages, most RPE cells in the fluorescent region were labeled, but the extent of expression was limited. In four RCS rats examined 3 days after Ad-*GFP* injection, fluorescent RPE cells were found in 33, 33,

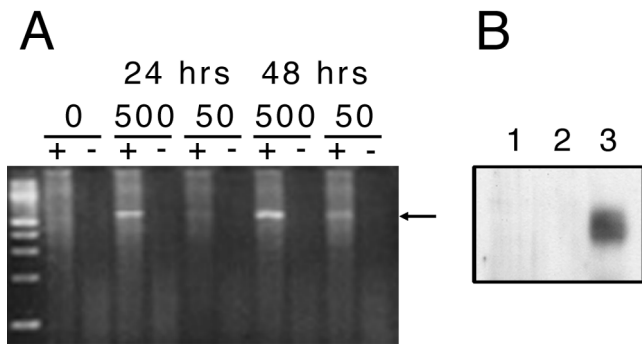


**Fig. 1.** *Ad-Mertk* expresses *Mertk* mRNA and protein in infected HeLa cells. (A) Cells were infected with different amounts (0, 50, or 500  $\mu$ l) of cell lysate containing *Ad-Mertk* for 24 or 48 h, and RNA was isolated. cDNA was synthesized in the presence (+) or absence (–) of reverse transcriptase. PCR was performed to detect a fragment of rat *Mertk* (arrow), and products were resolved by agarose gel electrophoresis. The left-most lane is a 100-bp ladder. (B) An immunoblot was performed on total protein from cells infected with (1) no virus, (2) *Ad-GFP*, or (3) *Ad-Mertk*, and probed with a polyclonal antibody directed against rat *Mertk*.

50, and 60% of the length of the RPE along the vertical meridian, restricted almost exclusively to the superior hemisphere where the injection was made. In contrast, a wider distribution of fluorescent RPE cells was seen with wild-type RCS-*rdy*<sup>+</sup> rats (Table 1, Exp. 3). In four wild-type rats examined 3 days after injection, fluorescent RPE cells were found in 50, 50, 100, and 100% of the length of the RPE.

RT-PCR was used to assess expression of wild-type *Mertk* in the neural retina and RPE/sclera of nine RCS rats 10 days after they were injected (at P23–P25) with the equivalent of 0.5 or 1  $\mu$ l of *Ad-Mertk* stock. Wild-type *Mertk* mRNA was detected in the RPE/sclera (8/9) and neural retina (7/9) of treated animals and was absent from uninjected controls (data not shown).

***Ad-Mertk* Rescues PRs.** In our initial experiment with *Ad-Mertk* (Table 1, Exp. 1), the appearance of the retina in the inferior

hemisphere of the eye, distant from the injection site in the superior hemisphere, was very similar to that of uninjected controls and characteristic of RCS rats at this age (30). The equatorial to peripheral retina had approximately one discontinuous row of PR nuclei in the ONL, highly attenuated RPE, and an intervening OS debris zone containing a number of macrophages (Fig. 2A). In the posterior region of the inferior hemisphere, the debris zone was eliminated from some focal regions of degenerated retina (Fig. 2B), as seen in the posterior retina of RCS rats at this age (30). By contrast, the superior hemisphere of treated eyes revealed preservation of PRs (Fig. 2C and D) in each of the animals. In some regions, the ONL contained two to four rows of PR nuclei with only very short PR inner segments and OS (Fig. 2C). In other regions, the outer retina appeared almost normal, with seven to eight rows of nuclei in the ONL and well-formed PR inner segments and OS (Fig. 2D). In regions with an intermediate number of nuclei (four to five rows), short disorganized OS were typically found. In some regions of some retinas, there was clear evidence of PR rescue, with two to four rows of nuclei, but an OS debris zone separated the surviving PRs and the RPE (not shown).

In two of the three injected eyes in the initial experiment, although small segments of the superior hemisphere showed substantial PR rescue, a large part of the superior hemisphere had an almost totally obliterated RPE, outer retina, and some of the inner retina, a phenomenon not observed in untreated RCS eyes. Through a series of experiments in which vehicle alone was injected into RCS or wild-type eyes, we attributed this effect to toxicity of the 10% glycerol used as a cryopreservative in the viral vehicle. Subsequent experiments were carried out either with *Ad-Mertk* diluted 1:10 in PBS (Table 1, Exp. 4 and 5), in which case the dramatic disruption of the retina was not seen, or dialyzed overnight against PBS (Table 1, Exp. 6), in which case little or no disruption was observed.

In the experiments with diluted or dialyzed *Ad-Mertk*, PR rescue was found in most of the experimental eyes (8/10 and 7/10 with the diluted and 4/10 with the dialyzed *Ad-Mertk*). In almost all cases, PR rescue was found only in the superior hemisphere, the same distribution as with the stock *Ad-Mertk*

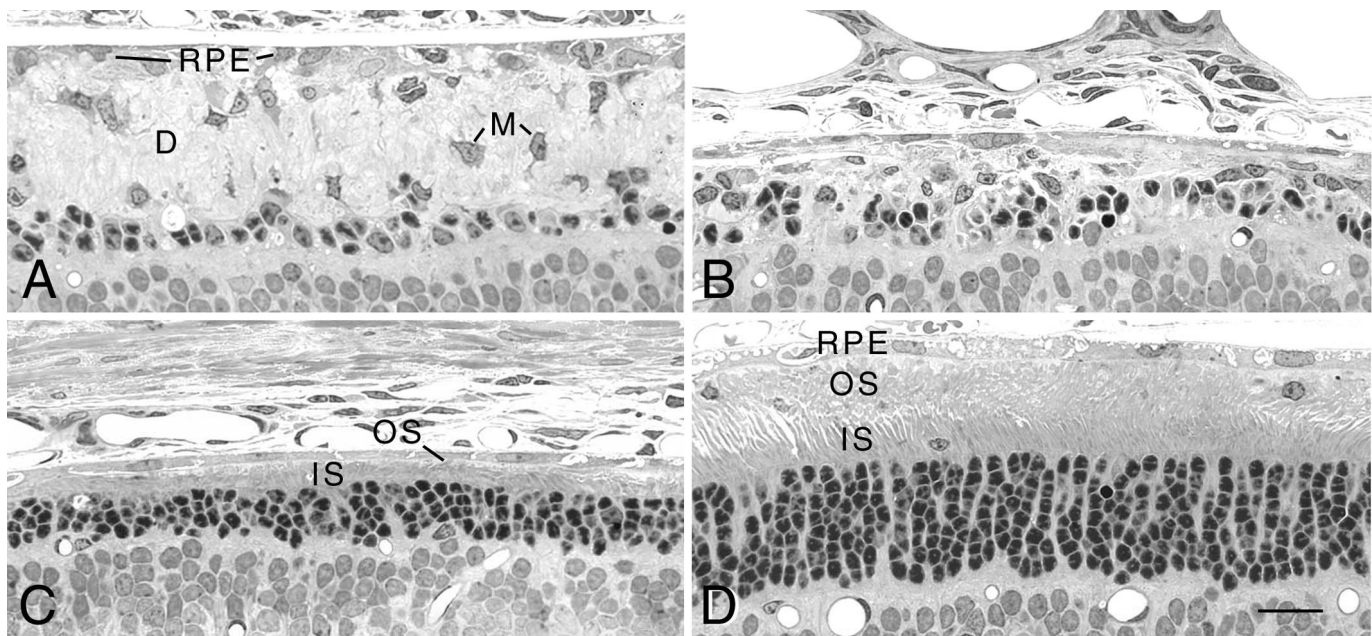


**Fig. 2.** Light micrographs of a single RCS rat retina injected in the superior hemisphere with *Ad-Mertk* at P22 and taken at P52. (A) Peripheral retina in the inferior hemisphere shows a thick OS debris zone (D) containing numerous macrophages (M). (B) Posterior retina in the inferior hemisphere. (C) Posterior retina in the superior hemisphere. (D) Peripheral retina in the superior hemisphere in the region of *Ad-Mertk* injection. (Bar = 20  $\mu$ m.)

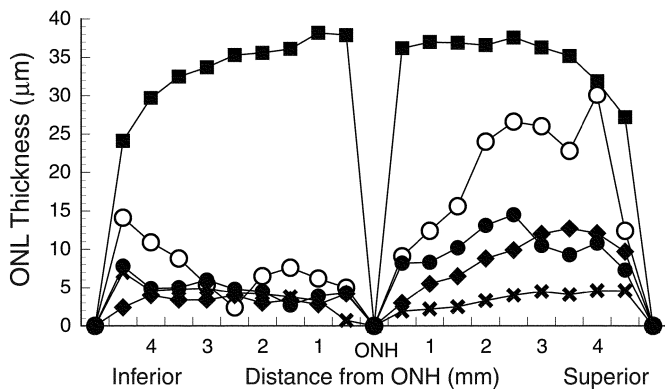


**Fig. 3.** Measurements of the ONL thickness along the vertical meridian of the eye from the optic nerve head (ONH) to the ora serrata of wild-type RCS-*rdy*<sup>+</sup> rats (■; *n* = 4) and retinal dystrophic RCS rats taken at P52-P57. To illustrate the distribution and magnitude of rescue, representative sections of eyes injected with either stock Ad-*Mertk* (○; *n* = 1), diluted Ad-*Mertk* (●; *n* = 7) or dialyzed Ad-*Mertk* (◆; *n* = 3) are compared with those of uninjected RCS rats (×; *n* = 3).

(Fig. 3). In a few eyes that showed no apparent rescue along the vertical meridian of the eye, deeper sectioning into the eye revealed some rescue. Thus, it is possible that some of the retinas reported as “no rescue” may have had focal preservation that we missed.

In the RCS rat retinas injected with Ad-*Mertk*, the magnitude of PR rescue (number of cells preserved) was greatest in the retinas injected with the stock virus. As shown in Fig. 3, one region of the retina showed almost 95% of the normal number of PRs when compared with a wild-type retina. The degree of rescue with the diluted and dialyzed Ad-*Mertk* most often appeared similar to that shown in Fig. 2C. However, the maximal rescue for a given retina was usually greater than that shown in Fig. 3, which averages each region of the retina for a number of animals, thus obscuring individual peaks of rescue in a given retina. When the single maximal ONL thickness measurement was tallied for each retina, five of the animals that received diluted virus and one that received dialyzed virus showed maximal ONL thickness measurements greater than 60% of that in wild-type rats. Maximal values were frequently greater than 40% of the wild-type value, whereas the maximal ONL measurements in uninjected and buffer-injected RCS rats were 30 and 28% of wild-type values, respectively.

In every experiment, the mean ONL thickness of the superior hemisphere (mean of 27 measurements in each eye) of Ad-*Mertk*-injected eyes was greater than that of the inferior hemispheres of the same eyes and of the superior hemispheres of vehicle-injected, PBS-injected, or uninjected eyes with a statistical significance of at least  $P < 0.05$ , and often  $P < 0.01$ . The mean ONL thickness of the nonrescued inferior hemisphere did not differ statistically from that of the uninjected or buffer/vehicle-injected control eyes, and these did not differ from each other. The mean (of 54 measurements across each eye) ONL thicknesses of eyes injected with diluted or dialyzed Ad-*Mertk* were significantly greater than those of controls ( $P < 0.005$ ).

**Reversal of RPE Phagocytosis Defect.** Failure of RCS RPE to phagocytize shed OS membranes leads to an early and rapid accumulation of OS debris at the apical surface of the RPE (4, 38). Thus, at the time of viral injection around P23, rod OS no longer reach the apical surface of the RPE (1, 4, 38). By contrast, 30 days after injection of Ad-*Mertk*, in areas of significant PR rescue, rod OS reach the apical surface of the RPE, without an intervening debris layer, as seen by light (Fig. 4 A and B) and electron (Fig. 4 C and D) microscopy.

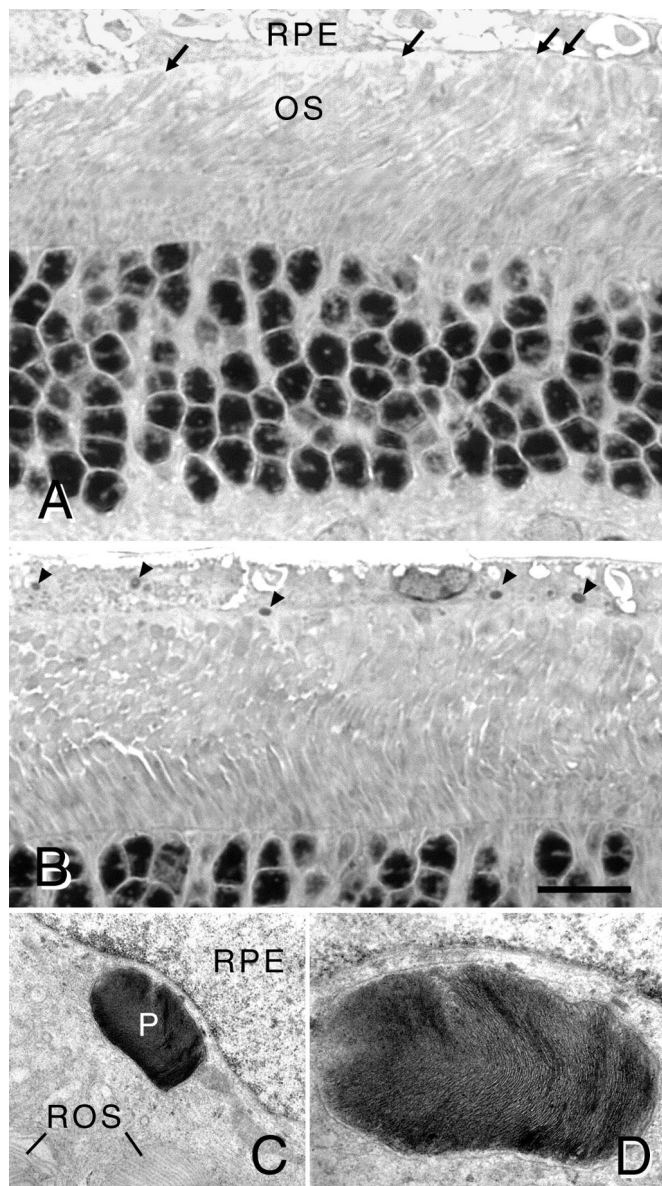


**Fig. 4.** (A and B) Light micrographs of retinal sections of an RCS rat at P52 that received stock Ad-*Mertk* at P22. (A) Tips of rod OS (ROS) reach the apical surface of the RPE (arrows). (B) Numerous phagosomes are present in the RPE cytoplasm (arrowheads), demonstrating ingestion of shed ROS membranes. (Bar = 15 µm.) (C and D) Electron micrographs of a retinal section comparable to that in B. (C) A large phagosome (P) is found in the cytoplasm and near the nucleus of an RPE cell. Tips of ROS are apposed to the apical surface of the RPE cell.  $\times 10,625$ . (D) Higher magnification ( $\times 28,600$ ) of a serial section to (C) illustrating ROS-like lamellar disk membranes within the phagosome.

The key phenotypic characteristic of mutant RCS RPE cells is failure to ingest shed OS membranes, resulting in few, if any, phagosomes in the RPE. Rod OS disk shedding follows a circadian rhythm in rats, with the peak of disk shedding occurring 1–2 h after the onset of light in the morning (39). To maximize the chance of seeing evidence of phagocytosis, we fixed the eyes of the rats that received stock Ad-*Mertk* (Exp. 1) during the presumptive peak of disk shedding. In all three rats, large phagosomes were found by light microscopy in the apical processes and cytoplasm of RPE cells (Fig. 4B), which appeared identical to those seen in normal wild-type rats (39). We confirmed by electron microscopic examination that the phagosomes were, in fact, lamellated packets of rod OS disk mem-

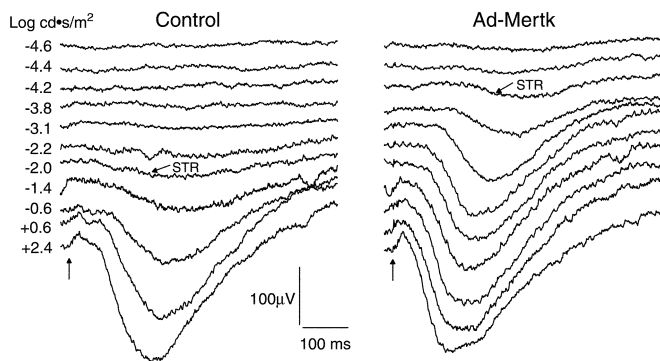


**Fig. 5.** Scotopic ERG intensity series from the uninjected eye (Left) and contralateral dialyzed Ad-Mertk-injected eye (Right) of an RCS rat at P60. Vertical arrows indicate application of the stimulus. Slanted arrows indicate STRs recorded at threshold stimulus intensity. The difference in the STR threshold between the control and treated eyes in this animal is greater than two log units.

branes (Fig. 4D) and that they were located within the RPE cell cytoplasm (Fig. 4C).

We counted the number of phagosomes in the RPE in rescued regions of two rats that received stock Ad-Mertk and obtained a mean of 7.3/field, a number about one-third to one-half that in normal albino rats. The eyes of rats that received diluted or dialyzed Ad-Mertk were fixed in the late afternoon (due to the constraints of ERG analyses), so the number of expected phagosomes in the RPE was low. Nevertheless, in several of these eyes, in regions where PR rescue was greatest, some large phagosomes were present in the RPE.

Infection of cultured RCS RPE cells with Ad-Mertk restores their ability to phagocytize exogenous OS to the level of wild-type RCS-*rdy*<sup>+</sup> cells (W.F., D.Y., M.T.M., M.M.L., and D.V., unpublished work), indicating that the RPE phagocytic activity we observe *in vivo* is a direct effect of *Mertk* expression.

**Increased Light Sensitivity Detected by ERG.** To determine whether functional rescue accompanied the retinal structural preservation, ERGs were measured at P55-P58 in some of the animals that received diluted or dialyzed Ad-Mertk (Table 1, Exp. 5 and 6). At P60, the ERG in pink-eyed RCS rats is characterized by the cornea-negative (1) STR (40), which originates in the inner retina and represents residual PR function in degenerating retinas (40, 41). The STR can be recorded in advanced degeneration where the a and b waves are unrecordable (41). STRs were recordable in all rats tested, but the maximal scotopic a and b waves did not exceed threshold levels. In seven of the nine rats examined that received diluted Ad-Mertk, there was no significant difference in STR threshold between treated and contralateral control eyes. In two rats, the STR threshold was 0.5 log units lower in the treated eye, consistent with a small improvement in retinal function in eyes treated with diluted *Mertk*.

In the 10 rats injected with dialyzed Ad-Mertk, however, the STR threshold was significantly lower than that in the contralateral control eyes by a mean difference of 0.82 log units ( $P = 0.02$ ; Fig. 5). The magnitude of this difference is similar to that seen in a neuroprotective treatment reported by others in RCS rats (42). Our results suggest that eyes treated with dialyzed Ad-Mertk had greater residual retinal function than contralateral control eyes.

## Discussion

Somatic gene transfer of *Mertk* to the retinas of RCS rats rescues PRs from degeneration and reverses the RPE phagocytosis defect. In regions near the injection site, numerous phagosomes

were found in RPE cells, and PR OS were apposed to the RPE apical surface, without intervening debris membranes. These features are never seen in RCS rats at the ages studied (4, 38). Our findings provide conclusive evidence that *Mertk* is the gene corresponding to *rdy* and substantiate a previous conclusion that *Mertk* is essential for the normal functioning of the mammalian retina (23), made on the basis of the RCS *Mertk* null mutation (14, 43) and discovery of *MERTK* mutations in individuals with retinitis pigmentosa (23). Our results suggest that treatment of patients with retinitis pigmentosa due to mutation of *MERTK* by viral-mediated gene therapy might be feasible; introduction of the gene into the eyes of juvenile rats, which already display significant pathology, resulted in areas of near normal-appearing retina.

Before the promise of human treatment can be realized, a great deal of further study will be necessary to accomplish widespread and prolonged correction of the phenotype. As part of this effort, it will likely be important to understand the factor(s) that limit the distribution of PR rescue, phagocytosis correction, and fluorescence of RPE cells (after Ad-GFP injection) to approximately a single hemisphere in RCS retinas. In studies with adeno-associated virus-vectored ribozymes delivered to PR cells in P23H mutant rhodopsin rats, the rescue effect was pan-retinal (29, 34). Likewise, when Ad-GFP was injected into normal control rats in the present study, RPE cells were transduced across the entire retina in some cases. One possible explanation for the restricted distribution in RCS rats is that the OS debris impedes diffusion of the injected agents, just as the debris has been suggested to impede the diffusion of metabolites and oxygen from the RPE to the retina. The debris may also prevent a bleb detachment as extensive as that in wild-type rats at the time of injection. Another possibility is that the increased surface area of the very long RPE cell processes (38), or perhaps of the debris membranes themselves, may bind the finite amount of injected reagent, thereby preventing its extensive diffusion. Viral injection in younger animals, in which little or no debris layer has accumulated, would begin to test these hypotheses.

There appeared to be a correlation between the degree of PR protection and the dose of Ad-Mertk. The stock virus had a greater effect than the diluted or dialyzed reagent, albeit at the cost of significant toxic effects of the 10% glycerol in the vehicle. Moreover, there appeared to be a gradient in the degree of PR protection from the injection site, where maximal rescue was seen, to regions where no rescue was seen. Use of a high-titer viral preparation free of glycerol is a logical next step toward improving the extent and magnitude of rescue.

The histologic appearance of the retina in Ad-Mertk-injected RCS rats ranged from virtually normal, with complete reversal of the genetic defect, to fully degenerated, typical of untreated RCS rats. Two intermediate phenotypes were seen that are not typical of RCS or wild-type rat retinas. Both phenotypes had two to four rows of PR nuclei, evidence of some PR protection, but very short or no OS and no debris zone in one case or a thin debris zone in the other case. The localization of these phenotypes surrounding more significantly rescued regions suggests a partial correction of the defect. Partial restoration of RPE phagocytosis could explain the case in which debris membranes are absent. The suboptimal PR rescue in such areas might have resulted from debris that was subsequently cleared by the time eyes were taken. The absence of significant OS in these regions precludes experimental demonstration of disk shedding and phagocytosis.

Several possibilities may lead to the phenotype in which a thin debris zone persists. Minimal transduction of some RPE cells could lead to a small amount of phagocytosis and persistence of debris. Alternatively, RPE cells in such regions may not have been transduced, but the debris zone may have been thinned, instead, by invading macrophages or, perhaps, by neighboring

fully transduced RPE cells. It is also possible that, at least near the injection site, the surviving PR cells may have been transiently protected by injection-induced injury, which can result in the persistence of some debris membranes (32). In either case, surviving PRs might be supported by adequate diffusion of metabolites through a thin debris zone or through adjacent areas that were more fully rescued. This mechanism of lateral support from neighboring cells was suggested as a possible explanation for the preservation of some PR cells underlying mutant RPE cells, but located near normal RPE cells, in both RCS rat chimera (3) and RPE transplantation experiments (44). Resolution of this issue awaits development of effective methods to detect Merck expression in the plastic sections required to see the thin debris zone.

Our study complements the recent remarkable demonstration of restoration of vision in a canine model of an RPE-based disorder by adeno-associated virus mediated transfer of *RPE65* (22), as well as an earlier study of mucopolysaccharidosis VII in mice by using an adenovirus vector (21). In these previous studies, the issue of neuronal degeneration could not be addressed because photoreceptor death did not occur during the experimental period. In the present study, we have provided the first example, to our knowledge, of correction of both an RPE

cell defect (phagocytosis) and accompanying PR cell degeneration. Taken together, these three studies not only serve as a proof of principle for restoring genetic function to the postnatal RPE, but they also demonstrate the relative ease and high efficiency of transduction of the RPE with a variety of virus vectors and in several different species. This bodes well for the development of gene-based therapy for retinal degenerations in which the defect is in the RPE. Moreover, the findings suggest that a gene-based approach may ultimately be appropriate therapy in the far more common age-related macular degeneration and allied disorders, in which a genetic etiology is increasingly more probable and cytopathological defects are seen in the RPE.

We thank Chenyi He for assistance in producing recombinant Ad-Merk, Jessica Weir for DNA sequencing, Ping Wu for ERG assistance, and Haidong Yang for fluorescence microscopy. This work was supported by a postdoctoral fellowship from the Fight For Sight Research Division of Prevent Blindness America (W.F.), K08 EY00415 (J.D.), DK49022 (M.A.K.), the Ruth and Milton Steinbach Fund and the Karl Kirchgessner Foundation (D.V.), by Grants EY01919, EY02162, and EY06842 from the National Institutes of Health, and by the Foundation Fighting Blindness, and by the Macula Vision Research Foundation (M.M.L.). M.M.L. is a Research to Prevent Blindness Senior Scientist Investigator.

- Dowling, J. E. & Sidman, R. L. (1962) *J. Cell Biol.* **14**, 73–109.
- Tamai, M. & Chader, G. J. (1979) *Invest. Ophthalmol. Visual Sci.* **18**, 913–917.
- Mullen, R. J. & LaVail, M. M. (1976) *Science* **192**, 799–801.
- Bok, D. & Hall, M. O. (1971) *J. Cell Biol.* **49**, 664–682.
- Chaitin, M. H. & Hall, M. O. (1983) *Invest. Ophthalmol. Visual Sci.* **24**, 812–820.
- Tso, M. O. M., Zhang, C., Abler, A. S., Chang, C.-J., Wong, F., Chang, G.-Q. & Lam, T. T. (1994) *Invest. Ophthalmol. Visual Sci.* **35**, 2693–2699.
- Herron, W. L., Riegel, B. W., Myers, O. E. & Rubin, M. L. (1969) *Invest. Ophthalmol.* **8**, 595–604.
- LaVail, M. M., Pinto, L. H. & Yasumura, D. (1981) *Invest. Ophthalmol. Visual Sci.* **21**, 658–668.
- Valter, K., Maslim, J., Bowers, F. & Stone, J. (1998) *Invest. Ophthalmol. Visual Sci.* **39**, 2427–2442.
- Bourne, M. C. & Grüneberg, H. (1939) *J. Hered.* **30**, 130–136.
- LaVail, M. M. (1981) *J. Hered.* **72**, 294–296.
- Ryeom, S. W., Sparrow, J. R. & Silverstein, R. L. (1996) *J. Cell Sci.* **109**, 387–395.
- Sparrow, J. R., Ryeom, S. W., Abumrad, N. A., Ibrahim, A. & Silverstein, R. L. (1997) *Exp. Eye Res.* **64**, 45–56.
- D'Cruz, P. M., Yasumura, D., Weir, J., Matthes, M., Abderrahim, H., LaVail, M. M. & Vollrath, D. (2000) *Hum. Mol. Genet.* **9**, 645–651.
- Lem, J., Flannery, J. G., Li, T., Applebury, M. L., Farber, D. B. & Simon, M. I. (1992) *Proc. Natl. Acad. Sci. USA* **89**, 4422–4426.
- Travis, G. H., Groshan, K. R., Lloyd, M. & Bok, D. (1992) *Neuron* **9**, 113–119.
- Bennett, J., Wilson, J., Sun, D., Forbes, B. & Maguire, A. (1996) *Nat. Med.* **2**, 649–654.
- Jomary, C., Vincent, K. A., Grist, J., Neal, M. J. & Jones, S. E. (1997) *Gene Ther.* **4**, 683–690.
- Takahashi, M., Miyoshi, H., Verma, I. M. & Gage, F. H. (1999) *J. Virol.* **73**, 7812–7816.
- Ali, R. R., Sarra, G. M., Stephens, C., Alwis, M. D., Bainbridge, J. W., Munro, P. M., Fauser, S., Reichel, M. B., Kinnon, C., Hunt, D. M., et al. (2000) *Nat. Genet.* **25**, 306–310.
- Li, T. & Davidson, B. L. (1995) *Proc. Natl. Acad. Sci. USA* **92**, 7700–7704.
- Acland, G. M., Aguirre, G. D., Ray, J., Zhang, Q., Aleman, T. S., Cideciyan, A. V., Pearce-Kelling, S. E., Anand, V., Zeng, Y., Maguire, A. M., et al. (2001) *Nat. Genet.* **28**, 92–95.
- Gal, A., Li, Y., Thompson, D. A., Weir, J., Orth, U., Jacobson, S. G., Apfelstedt-Sylla, E. & Vollrath, D. (2000) *Nat. Genet.* **26**, 270–271.
- LaVail, M. M. (1981) *Invest. Ophthalmol. Visual Sci.* **20**, 671–675.
- Bett, A. J., Haddara, W., Prevec, L. & Graham, F. L. (1994) *Proc. Natl. Acad. Sci. USA* **91**, 8802–8806.
- McGrory, W. J., Bautista, D. S. & Graham, F. L. (1988) *Virology* **163**, 614–617.
- Graham, F. L., Smiley, J., Russell, W. C. & Nairn, R. (1977) *J. Gen. Virol.* **36**, 59–74.
- Graham, F. L. & van der Eb, A. J. (1973) *Virology* **52**, 456–467.
- Lewin, A. S., Drenser, K. A., Hauswirth, W. W., Nishikawa, S., Yasumura, D., Flannery, J. G. & LaVail, M. M. (1998) *Nat. Med.* **4**, 967–971.
- LaVail, M. M. & Battelle, B. A. (1975) *Exp. Eye Res.* **21**, 167–192.
- Michon, J. J., Li, Z. L., Shioura, N., Anderson, R. J. & Tso, M. O. M. (1991) *Invest. Ophthalmol. Visual Sci.* **32**, 280–284.
- Faktorovich, E. G., Steinberg, R. H., Yasumura, D., Matthes, M. T. & LaVail, M. M. (1990) *Nature (London)* **347**, 83–86.
- Bayer, A. U., Mittag, T., Cook, P., Brodie, S. E., Podos, S. M. & Maag, K.-P. (1999) *Doc. Ophthalmol.* **98**, 233–246.
- LaVail, M. M., Yasumura, D., Matthes, M. T., Drenser, K. A., Flannery, J. G., Lewin, A. S. & Hauswirth, W. W. (2000) *Proc. Natl. Acad. Sci. USA* **97**, 11488–11493. (First Published September 26, 2000; 10.1073/pnas.210319397)
- Bennett, J., Wilson, J., Sun, D., Forbes, B. & Maguire, A. (1994) *Invest. Ophthalmol. Visual Sci.* **35**, 2535–2542.
- Li, T., Adamian, M., Roof, D. J., Berson, E. L., Dryja, T. P., Roessler, B. J. & Davidson, B. L. (1994) *Invest. Ophthalmol. Visual Sci.* **35**, 2543–2549.
- Akimoto, M., Miyatake, S., Kogishi, J., Hangai, M., Okazaki, K., Takahashi, J. C., Saiki, M., Iwaki, M. & Honda, Y. (1999) *Invest. Ophthalmol. Visual Sci.* **40**, 273–279.
- LaVail, M. M., Sidman, R. L. & O'Neil, D. A. (1972) *J. Cell Biol.* **53**, 185–209.
- LaVail, M. M. (1976) *Science* **194**, 1071–1074.
- Bush, R. A., Hawks, K. W. & Sieving, P. A. (1995) *Invest. Ophthalmol. Visual Sci.* **36**, 2054–2062.
- Sugawara, T., Sieving, P. A. & Bush, R. A. (2000) *Exp. Eye Res.* **70**, 693–705.
- Machida, S., Chaudhry, P., Shinohara, T., Singh, D. P., Reddy, V. N., Chylack, L. T., Jr., Sieving, P. A. & Bush, R. A. (2001) *Invest. Ophthalmol. Visual Sci.* **42**, 1087–1095.
- Nandrot, E., Dufour, E. M., Provost, A. C., Pequignot, M. O., Bonnel, S., Gogat, K., Marchant, D., Rouillac, C., Sepulchre de Conde, B., Bihoreau, M. T., et al. (2000) *Neurobiol. Dis.* **7**, 586–599.
- Li, L. & Turner, J. E. (1988) *Exp. Eye Res.* **47**, 911–917.